Review in Advance first posted online on August 17, 2016. (Changes may still occur before final publication online and in print.)

Uncertainty Quantification in Aeroelasticity*

Philip Beran,[1] Bret Stanford,[2] and Christopher Schrock[3]

[1]Multidisciplinary Science and Technology Center, Air Force Research Laboratory, Wright-Patterson Air Force Base, Ohio 45433; email: philip.beran@us.af.mil

[2]Aeroelasticity Branch, NASA Langley Research Center, Hampton, Virginia 23681; email: bret.k.stanford@nasa.gov

[3]Computational Sciences Center, Air Force Research Laboratory, Wright-Patterson Air Force Base, Ohio 45433; email: christopher.schrock@us.af.mil

Annu. Rev. Fluid Mech. 2017. 49:361–86

The *Annual Review of Fluid Mechanics* is online at fluid.annualreviews.org

This article's doi: 10.1146/annurev-fluid-122414-034441

Keywords

uncertainty quantification, aeroelasticity, polynomial chaos, flutter, limit-cycle oscillation, reliability, design under uncertainty

Abstract

Physical interactions between a fluid and structure, potentially manifested as self-sustained or divergent oscillations, can be sensitive to many parameters whose values are uncertain. Of interest here are aircraft aeroelastic interactions, which must be accounted for in aircraft certification and design. Deterministic prediction of these aeroelastic behaviors can be difficult owing to physical and computational complexity. New challenges are introduced when physical parameters and elements of the modeling process are uncertain. By viewing aeroelasticity through a nondeterministic prism, where key quantities are assumed stochastic, one may gain insights into how to reduce system uncertainty, increase system robustness, and maintain aeroelastic safety. This article reviews uncertainty quantification in aeroelasticity using traditional analytical techniques not reliant on computational fluid dynamics; compares and contrasts this work with emerging methods based on computational fluid dynamics, which target richer physics; and reviews the state of the art in aeroelastic optimization under uncertainty. Barriers to continued progress, for example, the so-called curse of dimensionality, are discussed.

1. INTRODUCTION

UQ: uncertainty quantification

LCO: limit-cycle oscillation

Aeroelastic responses are interactions among elastic structures (e.g., wings, structural panels, civil structures, turbine blades, and rigid bodies with elastic support), aerodynamic forces from the surrounding fluid, and inertia (Bisplinghoff et al. 1955). This review focuses on aircraft structures. From a computational perspective, uncertainty quantification (UQ) concerns itself with the quantitative estimation of all sources of uncertainty, including parametric uncertainty, model-form uncertainty, numerical uncertainty (Oberkampf & Roy 2010; C. Roy, private communication), and the predicted impact of these uncertainties on quantities of interest. UQ and aeroelasticity are important ingredients for the design optimization of more reliable aircraft.

There are numerous reasons for the UQ of aeroelastic systems that are perhaps more compelling than the UQ of either aerodynamic- or structural-only systems. First, aircraft need to be certified as free of dangerous aeroelastic instabilities in their flight envelopes, including a 15% equivalent airspeed margin (Nav. Air Syst. Command 1993). Although certification is not currently based on probabilistic measures, evaluating safety with respect to the presence of failure boundaries naturally introduces the notion of risk. Aeroelastic constraints are enforced in the preliminary design of aircraft and other structures. Designers can seek to minimize structural weight while meeting probabilistic safety constraints (design under uncertainty). Second, the UQ of aircraft aerodynamics may miss important physics if the body is assumed rigid; structural deformations are always present and influence, for example, shock behavior at transonic speeds. Finally, aeroelasticity involves many sources of uncertainty that can be difficult to disentangle, including measurement uncertainties during flight and ground testing, modeling and numerical uncertainties inherent to analysis methods, and uncertainties associated with how the aerodynamic and structural disciplines are modeled (e.g., failing to account for important physics in the transonic regime) and coupled (e.g., restricting interaction to certain surfaces).

1.1. Aeroelastic Physics

Aeroelastic physics are typically more challenging to predict than either fluidic responses about rigid bodies or structural responses under prescribed loads, given that coupling can introduce behavior not present in either discipline separately and that computed solutions can exhibit additional or altered length scales and timescales. Flutter and limit-cycle oscillation (LCO), which are self-excited, dynamic responses, are of primary interest in this article, owing to their importance to structural integrity and to the challenges of anticipating their dependence on uncertain inputs (see the sidebar Flutter and Limit-Cycle Oscillation). Other noteworthy aeroelastic phenomena include the following: static aeroelastic load redistribution of an elastic surface placed in an airstream; divergence, a static instability of that elastic surface (Bisplinghoff et al. 1955); whirl flutter, a dynamic instability associated with rotorcraft and propeller systems (Kunz 2005); stall flutter, a dynamic instability arising from a nonlinear relationship between aerodynamic loads and displacement at large angles of attack (Dowell 2015); buffet, an aerodynamically forced structural vibration [e.g., tail buffet exhibited by twin-tail aircraft configurations (Komerath et al. 1992)]; and dynamic responses of structures in gust.

1.2. Review-Oriented Literature

Whereas UQ and aeroelasticity separately have rich literatures, literature regarding their intersection is relatively sparse. This may be a result of several factors, such as the increased maturity of single-discipline studies, which provides a stronger analytical foundation for UQ investigations;

FLUTTER AND LIMIT-CYCLE OSCILLATION

Flutter and limit-cycle oscillation (LCO) are self-excited, temporal oscillations of the fluid-structure system. Flutter is a catastrophic, dynamic instability (Bisplinghoff et al. 1955). NASA's *Flutter at a Glance* film shows various forms of flutter (Reed 1981). LCO, or limit-cycle flutter (Bendiksen 2009), also arises from aeroelastic instability but is not divergent; oscillations grow until they reach a limited and sustained amplitude (Dowell et al. 2003). Flutter and LCO are often thought to arise from a Hopf bifurcation as parameters, such as dynamic pressure or Mach number, are varied (Morton & Beran 1999). Owing to the abrupt and divergent nature of flutter, it is normally associated with a point in a parameter space coincident with the Hopf bifurcation at which a change in dynamic stability occurs. In contrast, LCO amplitudes vary over a range of parameter values, depending on either the supercritical or subcritical nature of the bifurcation. There is also evidence that certain flutter instabilities do not conform to Hopf theory (Bendiksen 2006). From a Hopfian perspective, flutter and LCO have a common origin; however, the essential nonlinearities that limit the growth of limit cycles arise from different phenomena than those responsible for the loss of dynamic stability. This distinction is relevant to the construction of methods for propagating aeroelastic uncertainties.

the relatively high cost of carrying out aeroelastic analyses, especially owing to the typical need for conducting stability analysis; and the large number of potential uncertainty variables contributed by built-up aircraft structures.

Before proceeding, we differentiate between two branches of aeroelasticity: the traditional and widespread practice of aeroelasticity using aerodynamic models with fidelity lower than typically employed in computational fluid dynamics (CFD) and a newer practice of aeroelasticity based on CFD. We compactly designate these practices traditional aeroelasticisty (TAE) and computational aeroelasticity (CAE), respectively, and split much of the review along these lines.

Pettit (2004) provided an early review of UQ in aeroelasticity, emphasizing uncertainty categorization, the propagation of probabilistic inputs to stochastic flutter and LCO responses, design methods accounting for aeroelastic reliability, nonprobabilistic and nondeterministic (μ-analysis) methods for aeroelastic analysis and design, uncertainty in aeroelastic tests, research needs for advancement of UQ in aeroelasticity, and application of UQ to decision making. Although Pettit commented relatively little on UQ in CAE, he provided examples of UQ in TAE with nonlinear responses, pointed to the then-recent application of stochastic spectral methods to CFD, and discussed computational issues of meshing and discipline coupling as challenges for UQ.

Pettit's (2004) review was followed by others of differing scope. Beran et al. (2006) reviewed progress in representing stochastic, time-dependent, aeroelastic responses, focusing on a general comparison of three sets of methods: large-time, stochastic expansions of TAE responses using Hermite polynomials and Haar wavelets; Hermite expansions of cyclic solutions well suited for LCOs; and B-spline stochastic projections of two-dimensional (2D) CAE solutions (Millman 2004). Although this review addressed aerodynamic and structural sources of nonlinearity including some CFD solutions, the sources of uncertainty considered were primarily parametric in nature and of low dimension. Badcock et al. (2011) first reviewed UQ in aeroelasticity from a primarily CFD perspective, drawing on prevailing advances in CAE methods for flutter analysis based on a Schur complement strategy, a multifidelity Kriging framework for estimating values of the Schur interaction matrix (Timme 2010) and reducing modeling uncertainties, probabilistic and nonprobabilistic methods for propagating parametric uncertainties, and model-reduction techniques to enable efficient estimation of distributions of nonlinear responses. Beran & Stanford (2013) returned to an TAE perspective, focusing on methods to compute the probability

TAE: traditional aeroelasticity

CAE: computational aeroelasticity

of failure (POF) in aeroelastic systems, based on sources of uncertainty residing in the structure and its boundary conditions. Finally, Dai & Yang (2014) summarized in detail μ-analysis methods for aeroelastic analysis, design, and testing. Here a broad range of input uncertainties is described, including those arising from structural and aerodynamic models, although only within an TAE context. Several dissertations provide surveys of UQ in aeroelasticity (e.g., Millman 2004, Witteveen 2009, Khodaparast 2010, Riley 2011).

POF: probability of failure

MCS: Monte Carlo simulation

PC: polynomial chaos

PDF: probability density function

RV: random variable

There are many separate reviews of aeroelasticity and UQ in CFD. Three excellent reviews in aeroelasticity were published in 2003 (Dowell et al. 2003, Friedmann & Hodges 2003, Livne 2003). Dowell et al. (2003) and Livne (2003) targeted fixed-wing vehicles, addressing progress in CAE, including the simulation of transonic flutter and LCO [Livne (2003) provided some discussion of UQ in aeroelasticity as well]. Friedmann & Hodges (2003) reviewed the fundamental principles regarding aeroelastic phenomena of rotorcraft, focusing on stability. Surveys of UQ in CFD include two noteworthy reviews in this journal (Roache 1997, Najm 2009), with the latter treating spectral stochastic expansions that are relevant to this work. In a recent book, Bijl et al. (2013) addressed numerous specialized topics, including the treatment of physical discontinuities in a stochastic context and the use of sensitivities to enable the adaptation of response surfaces for efficient UQ.

1.3. Uncertainty Quantification Formulation Basics

In this article, a wide range of techniques are referenced for the propagation of uncertainties through aeroelastic systems, including Monte Carlo simulation (MCS), reliability methods, and perturbation methods. These UQ methods are fairly well known, and the reader is referred to the relevant citations for mathematical details beyond the cursory descriptions given below. More detailed treatments are given in this section for probabilistic approaches implemented with stochastic spectral expansions based on the polynomial chaos (PC) method (Section 1.3.1) or stochastic collocation methods (Section 1.3.2). A detailed formulation is warranted given the relative novelty of these methods, as well as their usefulness in complex CFD-based systems. Both classes of methods are typically utilized for uncertainties whose probability density functions (PDFs) are assumed known.

We emphasize that the input PDFs are often not well characterized, which might call into question the utility of a probabilistic approach. However, even low-order moments of PDFs can be informative, and probabilistic methods have the benefit of enabling uncertainties to be propagated in a manner that is valuable for system optimization, and they provide a framework by which epistemic uncertainties can be injected probabilistically. Owing to space limitations, the subject of quantifying input uncertainties is not considered further.

1.3.1. Spectral expansions. The general strategy of a spectral expansion is to develop a stochastic surrogate model dependent on random input parameters, which can be efficiently interrogated via probabilistic or nonprobabilistic sampling to efficiently quantify output statistics. Various spectral expansion techniques extend the PC-based, stochastic finite element method popularized by Ghanem & Spanos (1991) for solid mechanics. These are described in many places; the reader is referred to the review by Najm (2009) and articles by Barth (2013) and Eldred & Burkardt (2009) for many important details not described in this article.

A response or objective of interest, $w(\mathbf{x})$, can be globally approximated as a truncated expansion of $P+1$ weighted basis functions of n random variables (RVs), $\boldsymbol{\xi} = \{\xi_1, \xi_2, \ldots, \xi_n\}$:

$$w(\mathbf{x}, \boldsymbol{\xi}) = \sum_{k=0}^{P} \hat{w}_k(\mathbf{x}) \Psi_k(\boldsymbol{\xi}), \tag{1}$$

where w is a dependent variable (e.g., wing-tip displacement or flutter speed), and $\mathbf{x}$ is a set of independent variables (e.g., time and space coordinates or design parameters). Equation 1 serves as a stochastic surrogate model, linking random input quantities to outputs, and provides a flexible formulation that partitions the dependence on the random and independent variables into the basis functions and expansion coefficients, respectively.

PCE: polynomial chaos expansion

If the coefficients, $\{\hat{w}_k\}$, are known, Equation 1 can be easily interrogated to estimate, for example, response statistics. The expansion contains $P + 1 = (n + p)!/n!p!$ unique terms (Najm 2009) arising from a complete set of product and multidimensional cross-product terms of $\{\xi_k\}$ through order p, called the total-order expansion by Eldred & Burkardt (2009). The expansion in Hermite polynomials is referred to as the polynomial chaos expansion (PCE). Formulas for $\Psi_k(\xi)$ are provided in the literature cited above.

The expansion coefficients $\{\hat{w}_k\}$ can be computed by exploiting basis function orthogonality: $\langle \Psi_i, \Psi_j \rangle \equiv \int \Psi_i(\boldsymbol{\xi})\Psi_j(\boldsymbol{\xi})\rho_\xi(\boldsymbol{\xi})\mathrm{d}\xi = \delta_{ij}\langle \Psi_i, \Psi_i \rangle$, where δ_{ij} is the Kronecker delta, $\rho_\xi(\boldsymbol{\xi})$ is the PDF of the RVs, $\boldsymbol{\xi}$, and $\langle \cdot, \cdot \rangle$ is the inner product. For the Hermite polynomials, orthogonality is with respect to the Gaussian probability measure $\rho_\xi(\xi_i) = \frac{1}{\sqrt{2\pi}} e^{-\xi_i^2/2}$, where $\{\xi_i\}$ are normal Gaussian RVs ($\xi_i \in \mathbb{R}$) and $\langle \Psi_i, \Psi_i \rangle = i!$. Through a Galerkin-like spectral projection of Equation 1 onto the basis functions, orthogonality yields

$$\hat{w}_k(\mathbf{x}) = \frac{\langle w, \Psi_k \rangle}{\langle \Psi_i, \Psi_i \rangle} = \frac{1}{\langle \Psi_i, \Psi_i \rangle} \int w(\mathbf{x}, \boldsymbol{\xi})\Psi_k(\boldsymbol{\xi})\mathrm{d}\xi. \quad (2)$$

The so-called intrusive computation of $\{\hat{w}_k\}$ involves a spectral projection of the deterministic equations, leading to an expanded system of equations for $\{\hat{w}_k\}$, whose solution generally involves a significant modification of the deterministic methodology (typically the computer code) with a concomitant increase in computational cost and complexity. Uncertain physical parameters are associated with the RVs of the spectral expansion; for example, a structural stiffness may be designated $k = k_0 + k_1\xi$, where ξ is a normal Gaussian RV and k_0 and k_1 are the assumed mean and standard deviation of the stiffness distribution. Two relevant examples of this approach are reported by Le Maître et al. (2001) (the unsteady Navier-Stokes equations in two space dimensions) and Millman et al. (2005) (TAE-based LCOs of an airfoil with nonlinear structural coupling).

The intrusive approach has become less popular than the nonintrusive approach, a versatile, black-box strategy based on the collection of solution samples to numerically estimate the numerator of Equation 2. Eldred & Burkardt (2009) pointed to three general strategies—sampling (e.g., nondeterministic MCS), tensor product quadrature, and Smolyak sparse grids—indicating that the last is more efficient for larger random spaces. Point collocation is a different approach involving the least-squares computation of expansion coefficients by sample substitution into Equation 1 (Hosder et al. 2008).

Xiu & Karniadakis (2002) proposed a generalized PC approach including polynomials different than Hermite, orthogonal with respect to PDFs of non-Gaussian RVs, and using a potentially different basis for each RV. They demonstrated that spectral expansions matching the response distributions in each RV (which are not known a priori for general problems) led to exponential convergence and were optimal over the selection of any other expansion. However, for responses that exhibit sharp features in the parameter space, global expansions may be very inefficient (Millman 2004), a situation motivating the use of collocation methods (Section 1.3.2). Such features can arise from the switching of modes participating in flutter, as discussed in Section 2.

The generalized PC approach permits decoupling of the multidimensional integrals appearing in Equation 2 so that a basis-appropriate orthogonality can be exploited for each dimension (Eldred & Burkardt 2009). A mapping of the random space is employed to enable this property. The output is now considered to be expressed as $w(\mathbf{x}, \mathbf{r}) = w(\mathbf{x}, \boldsymbol{\xi})$, where $\mathbf{r}$ are the RVs in the

original problem, $\boldsymbol{\xi} = T(\mathbf{r})$ are the RVs in a standard normal space, and T is an appropriate nonlinear transformation. Eldred & Burkardt (2009) proposed several different transformations. The transformation of the stochastic domain is a key principle used in the reliability calculations described in Section 4.1.

1.3.2. Stochastic collocation. In contrast with the use of samples to compute coefficients of global spectral expansions, stochastic collocation methods use samples to determine the interpolating functions that form the surrogate. Barth (2013) described a product-based, multidimensional expansion of the form

$$w(\mathbf{x}, \boldsymbol{\xi}) = \sum_{i_1=1}^{m_1} \cdots \sum_{i_n=1}^{m_n} \hat{w}_{i_1,\ldots,i_n}(\mathbf{x}) \Psi_{i_1}(\xi_1) \ldots \Psi_{i_n}(\xi_n), \tag{3}$$

where m_i are the number of collocation points in each random direction, and $\Psi_i(\xi)$ are 1D bases obtained from Lagrange interpolation through the collocation points.

Millman (2004) and Millman et al. (2006b) applied a similar expansion to bulk aeroelastic responses (e.g., a peak angle of attack) involving two RVs using multivariate B-splines of the form $\Psi_{i_1}(\xi_1) = B_{i_1,k_1,\mathbf{x}_1}(\xi_1)$ and $\Psi_{i_2}(\xi_2) = B_{i_2,k_2,\mathbf{x}_2}(\xi_2)$, where $B_{i_1,k_1,\mathbf{x}_1}(\xi_1)$ is a univariate B-spline for the ξ_1 random direction of order $k_1 = 2$ with m_1 knots at $\mathbf{x}_1$ (and similarly for the ξ_2 direction). These B-splines provided a compact support, eliminating oscillations in the vicinity of discontinuities arising from bifurcations in aeroelastic response. Millman (2004) explored localized refinements of B-spline surrogates that achieved sharper resolution of bifurcations, as seen in **Figure 1*a***.

Dwight et al. (2013) employed an adaptive collocation procedure based on Newton-Cotes quadrature on simplex elements, an approach that enables costly solution samples to be recycled for computations on neighboring elements and regions of steep gradients to be resolved. The expected value of a response, $\langle w(\mathbf{x}) \rangle$, is estimated with this approach by

$$\langle w(\mathbf{x}) \rangle = \int w(\mathbf{x}) \rho(\xi) \mathrm{d}\xi = \sum_{i=1}^{N_\Omega} w(\mathbf{x}) \rho(\boldsymbol{\xi}) \mathrm{d}\xi \approx \sum_{i=1}^{N_\Omega} \sum_{j=1}^{N_\mathrm{q}} \hat{w}_{i,j} w_{i,j}(\mathbf{x}), \tag{4}$$

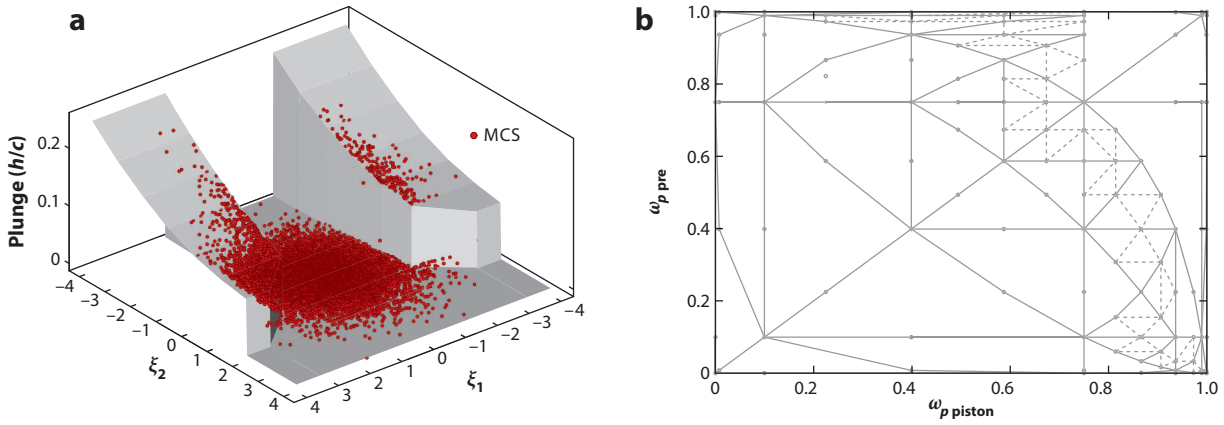

Figure 1

(*a*) Refined B-spline stochastic collocation of airfoil aeroelastic plunge response in limit-cycle oscillation with Monte Carlo simulation samples (where the plunge, h, is the vertical displacement normalized by the airfoil chord, c). Panel *a* adapted from Millman (2004). (*b*) Adaptive simplex elements for the piston problem subject to uncertainty in piston speed and initial pressure. Panel *b* adapted from Dwight et al. (2013) with permission of Springer.

where the space of RV support is subdivided into N_Ω elements, each discretized with N_q quadrature points, $\hat{w}_{i,j}$ are the quadrature weights of element i, and $w_{i,j}$ is the value of mode i at quadrature point j. **Figure 1*b*** shows the arrangement of simplex elements evolving during the simulation of piston-driven flow, subject to uncertainty in two parameters.

1.4. Article Road Map and Scope

This review first examines UQ in aeroelasticity from a traditional perspective using aerodynamic models of lower fidelity than either the Euler or Navier-Stokes equations (Section 2). This section alerts the reader to basic challenges in quantifying uncertainties in these TAE models, which are often (but not always) linear. Then, attention is turned to aeroelastic behaviors solved numerically with CFD (Section 3). This review establishes connections between recent research on UQ for CAE and a more extensive literature on the UQ of CFD-based aerodynamics, and exposes new challenges arising from the inclusion of higher-fidelity models. After establishing a foundation for how uncertainties in analytical responses are quantified, we next review the practical significance of this capability within the context of multidisciplinary design optimization (Section 4). This is consistent with our view that the introduction of uncertainty should inform the design of structures for reliable operation under air loads. Concluding remarks focus on the challenges of UQ in TAE and CAE and potential ways to address them (Section 5).

We limit our scope to aircraft aeroelasticity. Many important and relevant studies lie outside this scope owing to the physical problem, such as UQ in the aeroelastic response of civil structures (Caracoglia 2013), UQ in fluid-structure interactions at low Reynolds numbers (Xiu et al. 2002), and UQ in the aeroelasticity of rotorcraft (Murugan et al. 2008). Similarly, certain nondeterministic methods are excluded. Generally, this review focuses on probabilistic methods used to propagate parametric uncertainties in an aeroelastic context. Sources of modeling uncertainty are important and alluded to, but the quantification, propagation, and minimization of such uncertainties are not systematically addressed.

2. UNCERTAINTY QUANTIFICATION IN TRADITIONAL AEROELASTICITY

Time-dependent aeroelastic systems may be mathematically partitioned into equations for the aerodynamic ($\mathbf{w}_a$) and structural ($\mathbf{w}_s$) unknowns:

$$\begin{Bmatrix} \dot{\mathbf{w}}_a \\ \dot{\mathbf{w}}_s \end{Bmatrix} = \begin{Bmatrix} \mathbf{R}_a(\mathbf{w}_a, \mathbf{w}_s, \mathbf{x}, \mathbf{r}) \\ \mathbf{R}_s(\mathbf{w}_a, \mathbf{w}_s, \mathbf{x}, \mathbf{r}) \end{Bmatrix}, \tag{5}$$

where $\mathbf{R}_a$ and $\mathbf{R}_s$ are residual vectors, and $\mathbf{x}$ and $\mathbf{r}$ are as defined above: system parameters (design variables) and RVs. Equation 5 may be solved iteratively (by computing $\mathbf{w}_a$ for a fixed $\mathbf{w}_s$, and then vice versa, until convergence is obtained), or monolithically. Certain CAE applications may also require the mesh movement as a third set of unknowns in Equation 5 (Farhat et al. 2003), although only TAE applications are summarized in this section.

TAE systems cannot capture shocks or separated flow over a wing, which may be important for transonic aeroelasticity (Marques et al. 2010). However, the reduced computational cost of lower-fidelity aerodynamic tools facilitates repeated function evaluations of Equation 5, enabling the application of more powerful design and UQ tools. Eigenvalues of the coupled Jacobian (Equation 6) are typically available for these smaller systems, and their migration with changes in

x can provide insight into the aeroelastic mechanisms involved:

$$\mathbf{J} = \begin{bmatrix} \partial \mathbf{R}_a / \partial \mathbf{w}_a & \partial \mathbf{R}_a / \partial \mathbf{w}_s \\ \partial \mathbf{R}_s / \partial \mathbf{w}_a & \partial \mathbf{R}_s / \partial \mathbf{w}_s \end{bmatrix} \equiv \begin{bmatrix} \mathbf{J}_{aa} & \mathbf{J}_{as} \\ \mathbf{J}_{sa} & \mathbf{J}_{ss} \end{bmatrix}. \quad (6)$$

Furthermore, if the aerodynamic model is steady (no dependence on time), is quasi-steady ($\mathbf{w}_a$ depends only on instantaneous wing motion, not on its time history), or exists in the frequency domain, then $\mathbf{w}_a$ may easily be written as a function of $\mathbf{w}_s$. This allows each aeroelastic eigenvalue to be directly traced to the structural vibration modes (wind-off) of the wing (Bisplinghoff et al. 1955).

2.1. Uncertainty Quantification of Canonical Traditional Aeroelastic Systems

Much of the current literature dealing with UQ in aeroelastic systems utilizes TAE methods (papers that utilize CAE are summarized in Section 3). A typical application area for UQ is the aeroelastic response of a sectional airfoil elastically restrained in pitch and plunge [see early papers by Beran & Pettit (2004), Pettit & Beran (2004), and Millman et al. (2005)]. A second common application area is a thin panel, subject to supersonic flow (computed with quasi-steady piston theory) over its upper surface (see Liaw & Yang 1991, Lindsley et al. 2006b, Lamorte et al. 2014). For each of these references, aeroelastic flutter and/or LCOs are critical outputs.

Many of these papers quantify the variability in aeroelastic response due to aleatoric uncertainties, such as airfoil spring stiffness or laminated panel stacking sequence. These types of parametric uncertainties, with a clear relationship between **r** and the residual vectors $\mathbf{R}_a$ and $\mathbf{R}_s$, may be accounted for using Monte Carlo sampling (Yi & Zhichun 2010), spectral expansions such as PCE (Beran & Pettit 2004), or perturbation methods (Liaw & Yang 1991, Lindsley et al. 2006a). Model-form uncertainties are typically more challenging, although Lindsley et al. (2006b) demonstrated a technique in which uncertain panel boundary conditions are captured via probabilistic torsional hinge springs. Riley et al. (2011) directly accounted for model-form uncertainty by considering various aeroelastic models, each with an associated probability based on expert opinion.

MCS, in particular, is likely only practical for TAE-based methods, given the number of samples needed for accurate statistics of the aeroelastic output. Several sampling strategy enhancements exist (Hammersley & Handscomb 1964), but application to CAE is still typically impractical. Perturbation methods and spectral expansions approximate the relationship between random inputs and outputs with local and global approximations (see Equation 1), respectively, and require far fewer function evaluations. Perturbation methods require higher-order gradients, however (Verhoosel et al. 2009), and the cost of PCE scales poorly with the number of RVs and the order of the expansion, as noted in Section 1. The cost of spectral expansions may be tempered through the use of gradient enhancement (Roderick et al. 2010) and sparse approximations (Blatman & Sudret 2010).

2.2. Uncertain Flutter Response of Traditional Aeroelastic Systems

The studies mentioned above consider relatively simple aeroelastic models. More realistic aeroelastic models representative of full wing configurations may be obtained by coupling a detailed finite element model of the structure to an aerodynamic panel tool, such as the doublet lattice method. The PK method is an industry standard for solving such a system (see the sidebar The PK Method).

Many papers account for the UQ of an aeroelastic wing structure via the PK flutter method. Kurdi et al. (2007), Georgiou et al. (2012), and Scarth et al. (2014) all developed relationships

THE PK METHOD

A common form of the PK method (Hassig 1971) is written as

$$\left\{(U^2/b^2)p^2\mathbf{M} + (U/b)p\mathbf{C} + \mathbf{K} - \rho U^2\mathbf{Q}(ik)/2\right\}\mathbf{u} = \mathbf{0},$$

where $\mathbf{u}$ is a vector of modal amplitudes, the analog to $\mathbf{w}_s$ in Equation 1. U is the flow speed, ρ is the flow density, b is a reference length, and $\mathbf{M}$, $\mathbf{C}$, $\mathbf{K}$, and $\mathbf{Q}$ are the generalized mass, damping, stiffness, and aerodynamic force matrices, respectively. The complex Laplace parameter is written as $p = g + ik$, where k is the reduced frequency, and g is the modal damping. Because aerodynamic forces, $\mathbf{Q}(ik)$, have been written in the frequency domain, aerodynamic motion is written as a function of structural motion, and there is no analog to $\mathbf{w}_a$ in the above equation.

The form of the PK method given above is a nonlinear eigenvalue problem, where each eigenpair $(p, \mathbf{u})$ may be tracked across changes in flow parameters. Flutter occurs when a complex eigenvalue crosses into the right-half plane (i.e., g becomes positive). Each term in the equation, except for the computed eigenpair, may be considered explicit functions of the uncertain parameters $\mathbf{r}$. The eigenpair (and the flutter point as well) is an implicit function of these parameters, a dependence that can be quantified via uncertainty propagation.

between structural parametric uncertainties (i.e., the skin thickness of a wing box) and stochastic flutter mechanisms. Khodaparast et al. (2010) considered uncertain structural damping parameters ($\mathbf{C}$), and Bansal & Pitt (2013) considered uncertain aerodynamic forcing terms ($\mathbf{Q}$), although these quantities are found to have less of an impact on flutter variability relative to structural parameters ($\mathbf{M}$ and $\mathbf{K}$). The same UQ methods discussed above are utilized by these authors as well. MCS, in particular, is still a viable tool: Despite the complex nature of the wing-box structures utilized here (relative to a simple airfoil section or panel), the computational cost is relatively low owing to the modal representation used (see the equation in the sidebar The PK Method), and the fact that aerodynamic forcing terms $\mathbf{Q}$ are tabulated once, off-line, as a function of k.

Eigenvalue migration in the PK equations with increases in dynamic pressure will typically lead to many flutter mechanisms. Only the first mechanism (i.e., that with the lowest dynamic pressure) is of practical consequence, as this instability will compromise the wing's structural integrity before the second flutter mechanism is ever encountered. However, changes in the parameters $\mathbf{x}$ or $\mathbf{r}$ may lead to a reordering of the flutter mechanisms, changing the identity of the critical instability. This can challenge the UQ process, as the flutter point may be a discontinuous function of $\mathbf{r}$. This concept is highlighted by Scarth et al. (2014), who identified disjointed flutter behavior and bimodal flutter statistics for composite wing structures with uncertain ply angles (**Figure 2**). Costly high-order PCEs are required to resolve this bimodal behavior, although lower-order PCEs may be developed in the separate flutter regions and then combined into a unified model. This latter option requires some a priori knowledge of where these regions lie in the parameter space, however. Perturbation and reliability methods, which rely on local approximations, will fail to give accurate results for the bimodal responses shown in **Figure 2**, although the localized approximations offered by stochastic collocation (Equation 3) may be satisfactory.

2.3. Uncertain Limit-Cycle Oscillation Response of Traditional Aeroelastic Systems

For TAE-based systems, the nonlinearities leading to LCO are usually restricted to the structural mechanics, as aerodynamic nonlinearities typically require CAE [although Sarkar et al. (2009) demonstrated TAE-based UQ with a low-order dynamic stall model]. Leading-order

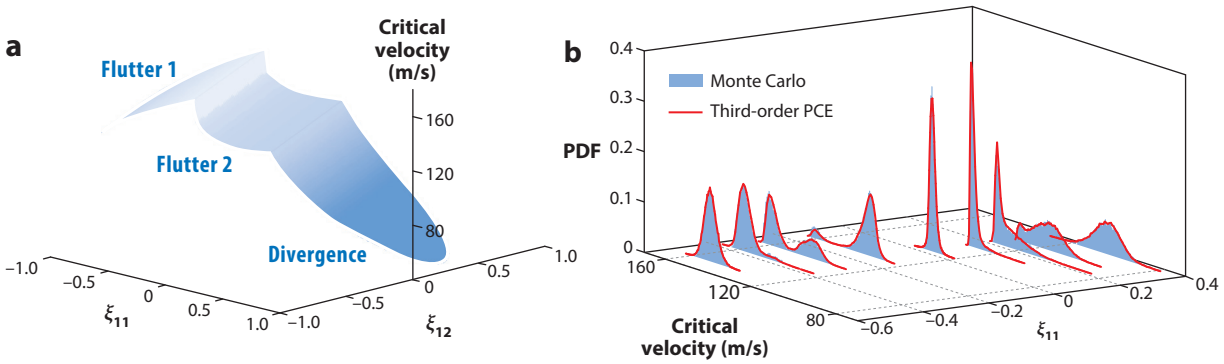

Figure 2

(*a*) Disjointed failure surface and (*b*) PDFs of the critical flutter speed for a range of laminated wing structure parameters. Figure adapted from Scarth et al. (2014), copyright Elsevier. Abbreviations: PCE, polynomial chaos expansion; PDF, probability density function.

nonlinearities that are stabilizing will lead to relatively benign supercritical LCOs at dynamic pressures beyond the flutter point, but destabilizing nonlinearities will cause dangerous subcritical LCOs, with stable, high-amplitude behavior on either side of the flutter point (Stanford & Beran 2013a). Fewer examples of the UQ of LCO behavior have been reported relative to linearized physics, owing to the higher cost and computational complexities.

LCOs may be computed by time integrating the nonlinear equations of motion (Equation 5) until the dynamics settle onto an orbit. Monte Carlo sampling (Attar & Dowell 2006, Yi & Zhichun 2010), perturbation methods (Castravete & Ibrahim 2008), and spectral expansions (Pettit & Beran 2004, Millman et al. 2005) have all been used to quantify the uncertainty of the time-integrated LCO (e.g., root-mean-square quantities). Alternatively, direct normal-form methods, which distill the leading-order nonlinear physics down to a few parameters (Ghommem et al. 2010), or time-periodic methods, which bypass initial transients in favor of monolithic-time orbits (Beran & Pettit 2004, Hayes & Marques 2015), may be used to reduce computational cost. These methods may be preferred for the UQ of subcritical LCOs, whose unstable orbits complicate the use of time integration.

Finally, discontinuities (or bimodal responses) may be found in the LCO parameter space, further complicating UQ efforts. This may arise from switching of the LCO's underlying linearized flutter mechanism, or a nonlinear transition from subcritical to supercritical behavior. Similar to the flutter results shown in **Figure 2**, Attar & Dowell (2006) demonstrated a multiregion response surface fit to quantify these types of LCO uncertainties.

3. UNCERTAINTY QUANTIFICATION IN COMPUTATIONAL AEROELASTICITY

Physical phenomena critical to the accurate prediction of aeroelastic behavior may require the employment of CAE-based methods. Such phenomena typically arise from nonlinearities in the governing equations (part of $\mathbf{R}_a$ in Equation 5) not accounted for in TAE models. Typical examples of such phenomena include the appearance of a transonic shock wave, separated flow, or both. These mechanisms can drastically alter the aeroelastic response of the system.

The development of CAE tools is itself an active area of research, with the computation of flutter and LCO a particular challenge. CFD methods are typically cast in the time domain, so flutter computations may involve repeated time integration analyses at increasing dynamic pressures, in

order to bracket the instability point. As g vanishes at the flutter point, dynamics in this vicinity will develop very slowly, and the computational cost can become significant. The development of an LCO can be similarly slow and expensive.

Various methods, reviewed below, may be used to reduce these complications, but in general, the computational cost of CAE will be orders of magnitude higher than its TAE counterparts reviewed in Section 2. As such, nondeterministic UQ tools reviewed above (such as MCS) are currently too computationally demanding to be viable. Analytical sensitivities of CAE tools are also an active area of research (Mani & Mavriplis 2008); thus, UQ tools that rely on gradient information (perturbation methods, gradient-enhanced PCEs) may not yet be feasible. Furthermore, there is a stronger focus in the CAE-based UQ literature on parametric uncertainties defining the flow environment (angle of attack, α, Mach number, M) than was commonly considered in the TAE-based tools reviewed above.

Given the increased computational cost of CAE-based tools, many authors have utilized TAE-based tools to first identify critical parameters whose uncertainties have large contributions to the aeroelastic response (Kurdi et al. 2007, Marques et al. 2010). This sensitivity analysis allows a selection of a limited set of random variables to ensure a tractable UQ problem size. Care must be taken in applying such an approach, as low-fidelity analyses may fail to identify a critical parameter whose dependency cannot be resolved without a higher-fidelity model. Other authors have employed the use of reduced-order modeling techniques to limit the number of CAE simulations that must be computed while maintaining a high-fidelity model (Nikbay & Acar 2015). Such approaches seek to generate a low-dimensional data reduction of the full CAE model through training data. The reduced-order modeling can then be evaluated to estimate system responses at other points in the solution space. Typically, such approaches are suitable near regions for which full data are plentiful, but suffer from inaccuracies in regions of sparse data. For this reason, within a UQ framework, such approaches typically exhibit poor performance for parameters with high variability (Lucia et al. 2004).

3.1. Uncertain Flutter Response of Computational Aeroelastic Systems

As an alternative to flutter point bracketing, the aeroelastic equations may be cast in an eigenvalue form using the Schur method (see the sidebar The PK Method for Computational Aeroelasticity), which allows for direct flutter computations with CAE tools, similar to the PK method described in Section 2 for TAE-based systems. Marques et al. (2010) used this method to compute the uncertain flutter behavior of various CAE wing models via MCS, perturbation methods, and interval analysis.

Perturbation methods are well paired with Schur flutter techniques, as the precise flutter result is then amenable to accurate gradient computations. Marques et al. (2010) expanded the real and imaginary components of the eigenvalues obtained by the Schur method about the mean value of the uncertain structural parameters as $p \approx p(\hat{\mathbf{r}}) + \frac{\partial p}{\partial \mathbf{r}}(\mathbf{r} - \hat{\mathbf{r}})$, with the derivative evaluated at the mean values of the structural parameters, $\hat{\mathbf{r}}$. The PDFs of $\mathrm{Re}(p)$ and $Im(p)$ can then be estimated from this linear relationship and the assumed PDFs of the uncertain structural parameters, $\mathbf{r}$.

When only the range of possible eigenvalues encountered under uncertainty is of interest in order to identify extremes of possible behaviors, interval analysis provides a less computationally intensive means of UQ. In the interval analysis approach, a range is defined for each uncertain structural parameter, and an optimization problem is solved to find the resulting range of the critical eigenvalue (Marques et al. 2010).

Marques et al. (2010) applied these approaches to the Euler-based analysis of the aeroelastic response of the Goland wing (Beran et al. 2004a). Prior linear analysis led to the identification

THE PK METHOD FOR COMPUTATIONAL AEROELASTICITY

The PK method presented above was extended to CAE by Timme & Badcock (2010). Their frequency-domain approach linearizes Equation 5 about an equilibrium solution, $\mathbf{w}_{eq}$, a static aeroelastic solution for a specified Mach number, M, and air density, ρ. Specifying perturbations of the form $\mathbf{w}(t) = \mathbf{w}_{eq} + \epsilon \mathbf{q} e^{pt} (\epsilon \to 0)$, the state-space equations become an eigenproblem for the aeroelastic eigenvector $\mathbf{q} \equiv \{\mathbf{q}_a, \mathbf{q}_s\}^T$:

$$(\mathbf{J} - p\mathbf{I})\mathbf{q} = \left(\begin{bmatrix} \mathbf{J}_{aa} & \mathbf{J}_{as} \\ \mathbf{J}_{sa} & \mathbf{J}_{ss} \end{bmatrix} - p\mathbf{I} \right) \begin{Bmatrix} \mathbf{q}_a \\ \mathbf{q}_s \end{Bmatrix} = \mathbf{0}.$$

For $\dim(\mathbf{w}_a) \gg \dim(\mathbf{w}_s)$, they constructed a low-dimensional, nonlinear eigenvalue problem governing $\mathbf{q}_s$ using the Schur complement (for structures modeled in either physical or generalized form):

$$((\mathbf{J}_{ss} - p\mathbf{I}) + \mathbf{S}^c(p))\mathbf{q}_s = \mathbf{0}, \quad (\mathbf{S}^c(p) \equiv -\mathbf{J}_{sa}(\mathbf{J}_{aa} - p\mathbf{I})^{-1}\mathbf{J}_{as}).$$

The coupling matrix, $\mathbf{S}^c$, of Timme (2010) vanishes in the absence of aerodynamic loads and is dependent on p. Similar to the PK method for TAE, aerodynamic loads are assumed to be harmonic and undamped [i.e., $\mathbf{S}^c(p) \approx \mathbf{S}^c(ik)$]. Timme (2010) described various strategies to compute $\mathbf{S}^c \equiv -\mathbf{J}_{sa}\mathbf{F}_{as}$. For small problems, $(\mathbf{J}_{aa} - ik\mathbf{I})^{-1}\mathbf{F}_{as} = \mathbf{J}_{as}$ is directly solved with LU decomposition (over each column of $\mathbf{J}_{as}$); for large problems, implicit pseudo-time integration can be employed. Sets of coupling matrices $\{\mathbf{S}^c(ik_i)\}$ are precomputed for selected reduced frequencies, $\{k_i\}$, and Mach numbers, $\{M_i\}$. To estimate the flutter speed at a given altitude, the precomputed $\{\mathbf{S}^c(ik_i)\}$ are interpolated when solving the above equation until $\mathrm{Im}(p) = k$ and M and U are consistent. The use of the Schur form enables rapid uncertainty propagation of the flutter speed subject to structural variability via perturbation analysis (Marques et al. 2010) or response surfaces of different $\mathbf{S}^c$ coefficients, potentially computed using different aerodynamic models (Timme 2010). Related formulations include the linearized harmonic K method (Bhatia & Beran 2014, 2015), applied to high-order finite element discretizations, and perturbations of Hopf points computed from the fundamental eigenproblem $(\mathbf{J} - p\mathbf{I})\,\mathbf{q} = \mathbf{0}$ (Lindsley et al. 2006a) and applied to a panel with structural variability.

of seven important uncertain parameters modeled as RVs, which were included in the analysis: leading- and trailing-edge spar thickness, upper and lower skin thickness, and the areas of the leading-edge, center, and trailing-edge spar caps. The results demonstrated that the perturbation approach could identify the range of the real part of the critical eigenvalue in 0.7% of the wall clock time required by MCS, whereas the interval approach found the range in 5–16% of the MCS wall clock time. We note that interval analysis is also able to compute the skewness of the response PDF, which the perturbation method cannot.

PC methods have also been successfully applied to quantify the effects of uncertainty on transonic flutter predicted with CAE. Nonintrusive polynomial chaos (NIPC) methods, in particular, have become increasingly popular as they are easily applied without modification of the underlying solvers. Hosder et al. (2008) applied the NIPC approach and MCS to assess the impact of uncertainty in M and α on the aeroelastic response of the AGARD 445.6 wing (Yates 1988) using an Euler solver. The NIPC approach employed a collocation method for the evaluation of the PC expansion coefficients. Both M and α were modeled as uniform RVs with $M \sim U(0.8, 1.1)$, and $\alpha \sim U(-2.0°, 2.0°)$.

NIPC: nonintrusive polynomial chaos

Rather than use the direct flutter methods employed by Marques et al. (2010), Hosder et al. (2008) utilized time integration to compute the CAE response. Each time response output is fit

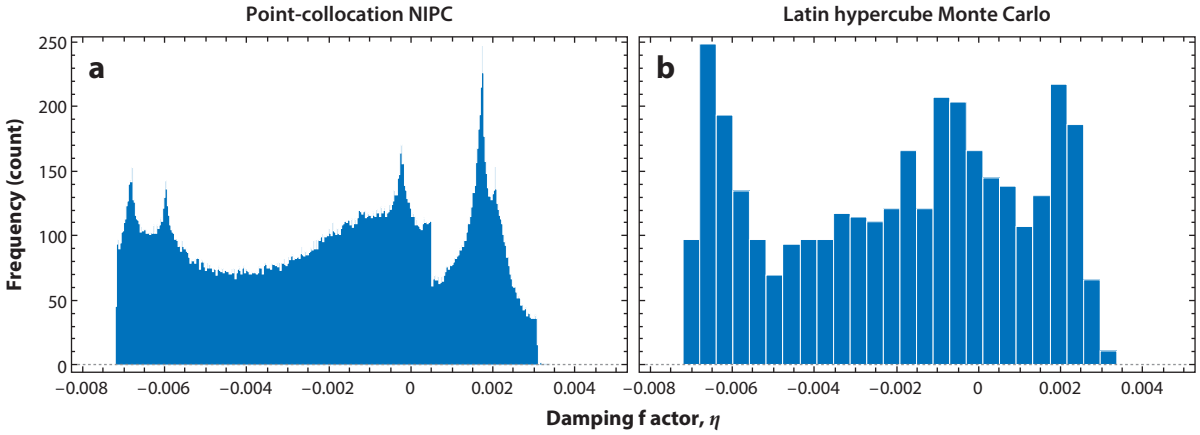

Figure 3

Histograms of the damping factor for the AGARD 445.6 wing with uniform uncertainty in M and α. (*a*) Eighth-order point collocation nonintrusive polynomial chaos (NPIC) approach and (*b*) Latin hypercube Monte Carlo simulation. Figure adapted from Hosder et al. (2008).

to the following function:

$$x(t) = a_0 + \exp(-\eta t)\left[a\cos(\omega t) + b\sin(\omega t)\right]. \tag{7}$$

Here, x represents a time-dependent response variable (e.g., generalized displacement/force) obtained through simulation, ω is the angular frequency, and η is the damping factor, with $\eta = -g$ used in Section 2. A value of $\eta = 0$ corresponds to the flutter point, and $\eta < 0$ is an unstable response. Histograms for the damping factor for this case are shown in **Figure 3**.

Although it is interesting that over this small range of flow parameters both damped and undamped aeroelastic responses are obtained, what is more intriguing is the highly irregular shape of the distribution of the damping factor. Hosder et al. (2008) attributed such an irregular response to uniformly varying input variables to aerodynamic nonlinearities, namely shock growth. We also noted that large polynomial degree expansions are required to facilitate the accurate representation of highly irregular distributions observed in this case. Hosder et al. (2008) concluded that, at an expansion degree of 8, all relevant statistics were sufficiently converged, falling within the 95% confidence interval of MCS. The NIPC method required 12, 30, 56, and 90 CAE runs for $p = 2$, 4, 6, and 8, respectively. Even at the highest order considered, the computational cost of the NIPC approach was an order of magnitude lower than MCS, though this was for only two uncertain parameters. If additional uncertain structural or material properties were included, the growing dimensionality of the problem may render an eighth-order NIPC approach impractical. It is also possible that additional uncertain parameters would further complicate the resulting distribution of the damping factor, requiring an even higher-order representation to maintain accuracy.

Beyond physical nonlinearities such as transonic shocks, various CAE numerical issues could contribute to irregular PDF responses, such as seen in **Figure 3**. These sources include the following: irregularities in mesh deformation resulting from aeroelastic wing shape changes; incomplete convergence in simulation time, leading to errors in damping estimation from Equation 7, particularly for the longest timescales resulting from the smallest damping values; incomplete convergence in time step; incomplete convergence between the structural and aerodynamic equations (Equation 5) at each time step; potential irregularities in the interpolation of loads and

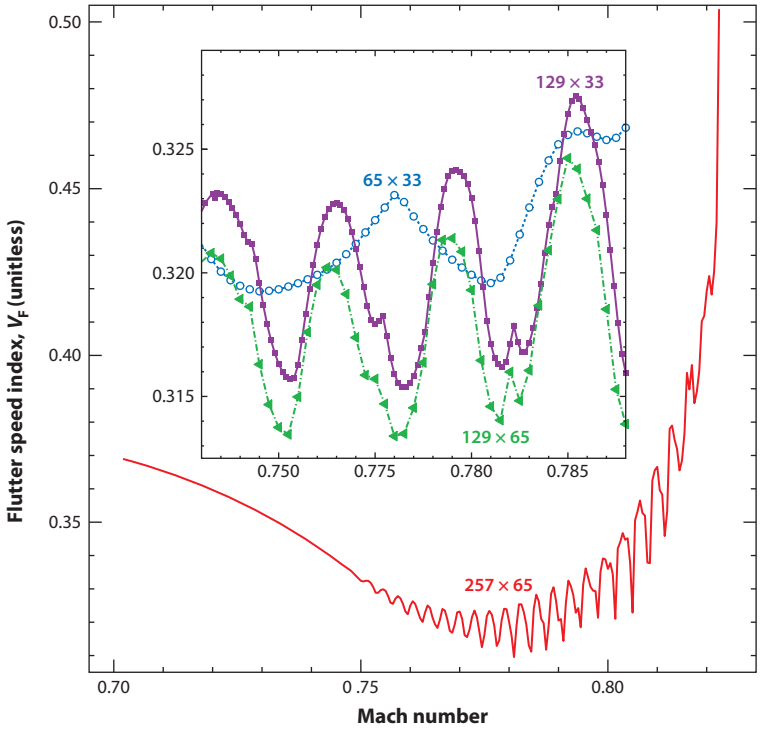

Figure 4

Jagged flutter boundary of a structurally supported NACA 0012 airfoil in the transonic regime for different meshes of C topology (number of streamwise grid points times the number of normal grid points). The flutter speed index is the reduced velocity normalized by the square root of the airfoil-to-fluid mass ratio. Specific definitions of these quantities for airfoils can be found in the aeroelasticity literature (e.g., Morton & Beran 1999). Figure adapted from Timme (2010).

displacements between the disciplines; and numerical consequences of potential nonsmooth shock motion in the aerodynamic analysis.

This last source was carefully studied by Timme & Badcock (2009), who computed the flutter boundary of a structurally supported NACA 0012 airfoil with a direct Schur method. The authors presumed this method to be free of time convergence, mesh deformation, and coupling-convergence problems. **Figure 4** shows a set of flutter boundaries computed by Timme & Badcock (2009) for a sequence of meshes, suggesting that the predicted flutter boundary becomes less smooth with grid refinement. Timme & Badcock (2009, p. 1592) attributed this effect to "the discrete displacement of the formed shock wave under variation of a particular system parameter." We have observed a similar phenomenon in the computed derivatives of the lift coefficient with respect to α ($C_{L\alpha}$) as a function of M for rigid airfoils. As the pitch-and-plunge equations representative of a structurally supported airfoil include $C_{L\alpha}$ as a source term, the two behaviors may be closely linked. The impact of such behavior on response characteristics collected in the manner shown in **Figure 3** is not known.

As noted above, PC methods suffer from the curse of dimensionality when a large number of RVs or large polynomial orders are required. The latter situation is particularly prevalent in CAE tools, whose nonlinearities lead to irregular PDFs (e.g., **Figure 3**). One solution may be to utilize the domain decomposition methods employed by Scarth et al. (2014) for PCEs

of multimodal responses (where the irregular PDF is caused not by physical nonlinearities, but by mode switching) summarized in Section 2. Sparse regularized approximations to Equation 1 (Blatman & Sudret 2010) and gradient enhancements (Roderick et al. 2010) may also be used to temper sampling costs.

Another possibility was proposed by Witteveen (2009), who provided a UQ framework with constant interpolation accuracy in time with a fixed number of samples known as unsteady adaptive stochastic finite elements (UASFE). The UASFE approach is similar to PC approaches in that it seeks to determine a representation of the dependence of the probability distribution of an RV over the probability space defined by the uncertainty variables. In this case, however, the representation is sought as a piecewise polynomial representation by subdividing probability space into multiple elements. Simplex elements are commonly employed. The formulation of the representation within each element is analogous to the PC approach, utilizing moment matching with quadrature employed to determine the unknown coefficients. Accuracy is improved by adaptively refining the elements based on the curvature of the approximate response, similar to the adaptive simplex element approach illustrated in **Figure 1*b***.

Witteveen (2009) presented results for the AGARD 445.6 wing with prescribed uncertainty in the free-stream velocity utilizing an Euler solver, where a reduction of three orders of magnitude in computational cost is observed with the UASFE method, relative to MCS.

3.2. Uncertain Limit-Cycle Oscillation Response of Computational Aeroelastic Systems

We now shift focus from the UQ of dynamical aeroelastic stability discussed in Section 3.1, which involves the study of linearized responses, to the UQ of LCO, which entails examination of nonlinear responses. The reader is referred to Section 2.3 for background concerning the formation of subcritical and supercritical LCOs and for a review of UQ literature regarding LCOs computed with TAE methods. Here, attention is on physical problems that warrant aeroelastic analysis with CAE methods.

An important and well-known example of aeroelastic LCO is exhibited by store-laden F-16s, which typically occurs in the transonic regime. F-16 LCO is often characterized by antisymmetric structural modes, along with lateral motion of the fuselage and cockpit, resulting in significant negative impact on aircraft operation (Bunton & Denegri 2000). Each store configuration must be certified, and allowable configurations permit the existence of LCO meeting a frequency-scheduled load-factor constraint within a defined flight envelope. Although the phenomenon is self-sustaining, its behavior may reflect hysteresis, its onset may "be self-induced or initiated by control inputs," and its amplitude can be sensitive to load factor (Bunton & Denegri 2000, p. 916). Another important source of sensitivity is store shape. Denegri et al. (2013) found that subtle aerodynamic variations in underwing missiles have a significant impact on LCO response levels.

The physics contributing to LCO can be uncertain. Although much attention has focused on aerodynamic mechanisms of LCO—specifically, shock-related phenomena in the transonic regime—some research points to contributions from nonlinear structural damping (Zhang et al. 2016). In particular, structural nonlinearity may explain the appearance of F-16 LCO when an effective aerodynamic quenching mechanism is not apparent (i.e., in certain subsonic situations in which shocks are largely absent, and in supersonic situations in which shocks are largely fixed to the edges and do not move over significant portions of the wing surface). Accurate quantification of aircraft structural nonlinearities is challenging; however, correlation with flight tests can yield computed LCO responses across the transonic regime with good agreement with observations (Zhang et al. 2016).

The CAE literature regarding the UQ of computed LCOs (i.e., the post-onset nonlinear behavior) is scant. One computational study of F-16 LCO presents limited results, documenting the sensitivity of the LCO amplitude to natural frequencies of two selected modes (8.2 Hz and 8.7 Hz) of the aircraft structure (Thomas et al. 2006). LCOs are computed with the harmonic balance method applied to the Euler equations for a geometrically complex configuration including tip and underwing stores. Small frequency alterations on the order of 4% (0.3 Hz), chosen to improve the alignment of flight test observations and computational predictions of flutter characteristics, led to the disproportionately large growth of the LCO amplitude in a manner more representative of flight responses. Thomas et al. (2006) noted that the difference between the frequencies of the first and second antisymmetric modes is 0.5 Hz, enabling the coalescence of modes that are a typical fingerprint of flutter to be sensitive to structural frequency.

Uncertainty propagation studies have been conducted for structurally supported airfoils immersed in inviscid, compressible flow. Millman et al. (2006a) examined an airfoil with third- and fifth-order nonlinear structural terms, whose coefficients were selected to produce subcritical LCOs. Owing to the structure of the bifurcation, discontinuous jumps in large-time aeroelastic response were exhibited in the deterministic problem. In their uncertainty study, two parameters were considered uncertain: the initial angle of attack, $\alpha(0) \sim N\,(0.0, 1.5°)$, and pitch cubic stiffness, $\beta_\alpha \sim N\,(-30.0, 3)$. Over the LCO hysteresis region, whose extent is dependent on β_α, the uncertainty in $\alpha(0)$ led to steady or LCO aeroelastic responses.

As described in Section 1, Millman et al. (2006a) employed a B-spline stochastic projection method using a structured sampling of the random space to construct response surfaces of different LCO quantities. Samples are large-time response values obtained from time integration. The uncertainty problem is to predict the POF, where failure is defined to occur if the LCO amplitude is too large or of too large a frequency. POF values are estimated by efficiently and randomly sampling the response surface. In comparison to MCS applied to the original system of equations, the stochastic projection method uses two–orders of magnitude fewer samples. Issues not addressed in the study include the following: quantifying method performance as the dimensionality of the random space increases, localized adaptations of the surrogate not calibrated to system behavior known a priori, broader parametric variations leading to a change of the global solution structure (e.g., from subcritical to supercritical), and couplings between the RVs arising from nontrivial values of static pretwist.

More recently, Hayes et al. (2014) also examined uncertainty propagation in the response of structurally supported airfoils. In their work, the Euler equations are solved with the harmonic balance method in a manner similar to that of Thomas et al. (2006), enabling efficient and precise characterization of the LCO response. The physical problem they posed produced supercritical LCOs. Several aerodynamic and structural variables are drawn from uniform, random distributions over specified intervals. Although little detail was given, apparently adaptive sampling was used to construct a PCE-based surrogate of the LCO solution, with particular attention to the point of bifurcation, where the local solution structure is strongly influenced by variability. Similar issues can be raised for this work as for Millman et al. (2006a), with the additional point that the efficiency enabled by harmonic balance precludes the consideration of variability in initial conditions, which may be important LCO triggers, as mentioned above regarding F-16 flight experiences.

4. AEROELASTIC OPTIMIZATION UNDER UNCERTAINTY

Having reviewed methods that enable the propagation of uncertainties through TAE (Section 2) and CAE (Section 3) systems, we now turn attention to methods by which these tools can inform

the design process. A deterministic design optimization problem may be written as

$$\min_{\mathbf{x}} \; f(\mathbf{x}) \qquad \text{s.t.} : \begin{cases} \mathbf{x}_{\min} \le \mathbf{x} \le \mathbf{x}_{\max} \\ \mathbf{g}(\mathbf{x}) \le \mathbf{0} \end{cases}, \tag{8}$$

RDO: robust design optimization

RBDO: reliability-based design optimization

where f is the objective function to be minimized, $\mathbf{x}$ is a vector of design variables (bounded by $\mathbf{x}_{\min}$ and $\mathbf{x}_{\max}$), and $\mathbf{g}$ is a vector of inequality constraints. For aeroelastic applications, f is often the structural weight, but may also be another quantity, such as aerodynamic drag. Design variables $\mathbf{x}$ commonly include structural variables (skin thickness, material properties), shape variables (airfoil definitions, planform shape), and control surface parameters. Constraints ($\mathbf{g}$) may be placed on, for example, maneuver stresses, skin buckling, the flutter speed, LCOs, and control authority.

The introduction of uncertainties into the deterministic Equation 8 is driven by two motivating factors. First, empirical safety factors are commonly built into the design constraints $\mathbf{g}$: 50% and 15% are typically used for stress and flutter metrics, respectively (Pettit 2004). A better defined margin of safety may be developed from knowledge of system uncertainties. Second, a system that minimizes f may be nonrobust. A preferable outcome is a design whose performance f is relatively unaffected by uncertainties (inherent either to the structure or to the surrounding flow). Therefore, a nondeterministic optimization problem may be stated as (Zang et al. 2002, Yao et al. 2011)

$$\min_{\mathbf{x}} \; \tilde{f}\left(\mu_f(\mathbf{x}, \mathbf{r}), \sigma_f(\mathbf{x}, \mathbf{r})\right) \qquad \text{s.t.} : \begin{cases} \mathbf{x}_{\min} \le \mathbf{x} \le \mathbf{x}_{\max} \\ P\left\{\mathbf{g}(\mathbf{x}, \mathbf{r}) \le \mathbf{0}\right\} \le \mathbf{P}_F \end{cases}. \tag{9}$$

The new objective function $\tilde{f}$ is computed from the mean (μ_f) and standard deviation (σ_f) of f. For example, it may be desirable to minimize $\mu_f + \sigma_f$. Each deterministic constraint has been replaced with a probability statement $P\{\cdot\}$, constrained to be less than some required failure probability $\mathbf{P}_F$. The inclusion of the probabilistic objective function and constraints is commonly referred to as robust design optimization (RDO) and reliability-based design optimization (RBDO), respectively (Yao et al. 2011). The parameters $\mathbf{r}$ are uncertain in Equation 9, and the design variables $\mathbf{x}$ may be as well. Situations with both probabilistic objectives and constraints have been referred to as R^{2}BDO (Paiva et al. 2014).

Tools used to solve Equation 8 or 9 may be broken into two categories: gradient-based and non-gradient-based optimization. The former repetitively computes derivatives of the objective and constraints with respect to $\mathbf{x}$ and then uses this information to move to another location in the design space. The latter comprises a wide range of tools, but all are derivative-free and most rely on global sampling. Furthermore, optimization tools may sample directly from the true design space, or from a surrogate model. All these choices have direct analogs with methods used for the UQ of $\mathbf{r}$ in Sections 2 and 3. The UQ analogs to gradient-based optimization are perturbation methods and reliability analyses, both of which require sensitivities. The UQ analog to surrogate-based design may be spectral expansions, which can be thought of as a global response surface of the uncertain parameters (Allen & Camberos 2009). If the design variables $\mathbf{x}$ are probabilistic, the two classes of tools (optimization and UQ) often require the same information.

4.1. Reliability-Based Design Optimization

For situations with a large number of design or uncertain variables, or very expensive analyses (such as CAE), often the only feasible option is gradient-based optimization, with the gradients computed via an analytical adjoint-based approach (see Mantegazza & Bindolino 1987 and Mani & Mavriplis 2008 for aeroelastic sensitivity formulations). For RBDO problems, the first-order reliability

THE FIRST-ORDER RELIABILITY METHOD

FORM estimates the POF by locating the most probable point along the failure surface $\mathbf{g}(\mathbf{x}, \mathbf{r})$ transformed into the independent standard normal random space $\mathbf{g}(\mathbf{x}, \xi)$. In this space, the distance between the origin and most probable point is the reliability index β. The POF is approximated as $\Phi(-\beta)$, where Φ is the cumulative distribution function of the standard normal distribution. This POF is exact if the failure surface is linear and ξ are jointly normal: Potentially large errors are introduced otherwise (Melchers 1987, Rackwitz 2001).

method (FORM) is a commonly used approach in the aeroelastic (and broader) literature (see the sidebar The First-Order Reliability Method).

FORM: first-order reliability method

Figure 5 shows an example from Stanford & Beran (2013b) for a thin metallic fluttering panel with uncertain leading- and trailing-edge torsional spring stiffness. Spring stiffness is assumed constant along each attachment line. Weibull distributions are assumed for both variables, ranging from zero (simply supported boundary conditions) to infinity (clamped). Using uncertain torsional springs as an analog for uncertain boundary conditions converts an epistemic uncertainty into a parametric one.

The nondimensional flutter speed is plotted in both physical space and standard normal space, along with a beta value of unity (i.e., the most probable point lies one standard deviation from the mean). The most probable point is located via derivatives of the flutter speed with respect to $\mathbf{r}$, with significant nonlinearities in the failure surface at this point. The POF (i.e., probability that the flutter speed will be less than the required threshold) is 15.9% as computed by FORM, and 12.4% as computed by MCS. Subsequently, the derivative of this POF with respect to $\mathbf{x}$ is easily computed for RBDO purposes (Stanford & Beran 2013b).

Allen & Maute (2004) and Nikbay & Kuru (2013) utilized Euler-based CAE for aeroelastic FORM-based RBDO to optimize a wing via structural design variables ($\mathbf{x}$) with uncertain material properties and flow conditions ($\mathbf{r}$), under probabilistic stress and cruise efficiency constraints. Allen & Maute (2005) incorporated planform shape design variables as well. Dynamic probabilistic

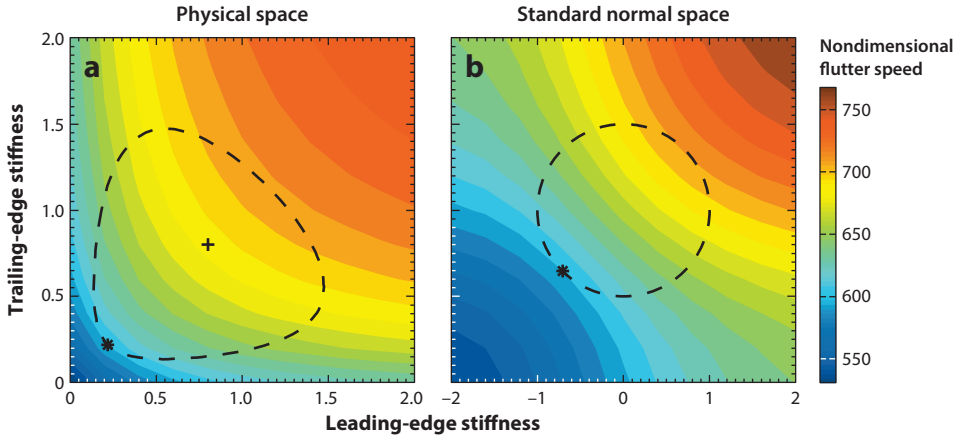

Figure 5

Nondimensional panel flutter speeds as a function of the leading-edge (LE) and trailing-edge (TE) torsional stiffness, in the (*a*) physical space and (*b*) standard normal space. The reliability index is indicated by a dashed line, the most probable point indicated by an asterisk. Figure adapted from Stanford & Beran (2013b).

aeroelastic constraints in the form of gust response, flutter, and LCOs were utilized by Pettit & Grandhi (2003), Stanford & Beran (2013b), and Stanford & Beran (2012), respectively, albeit using TAE systems.

SORM: second-order reliability method

The POF accuracy issues related to FORM may be improved through second-order derivatives [the second-order reliability method (SORM)], although this method has not, to our knowledge, been utilized for aeroelastic optimization, presumably because of the complexity involved in computing these terms. Verhoosel et al. (2009) demonstrated the SORM for a panel flutter problem, although not in an optimization context.

Another option is to approximate the failure PDF with a surrogate model, followed by a POF computation via the area within the tail. This POF is then used for RBDO, as demonstrated by Manan & Cooper (2009) via PCE, Scarth et al. (2015) using Gaussian emulators, and Missoum et al. (2010) with support vector machines, for flutter and LCO problems. Gradients of the surrogate model (for gradient-based optimization) may be computed from the derivative of the expansion coefficients, formulated by Eldred (2009) for nonintrusive PCE. A bimodal failure PDF (as noted in Scarth et al. 2015) will complicate the analytical gradient computations and may force the use of non-gradient-based optimization. Any random sampling process used to obtain the expansion coefficients $\hat{w}_k$ from Equation 1 will also complicate gradient-based optimization (Padulo et al. 2011).

Figure 6 shows sample RBDO results from Scarth et al. (2015) for the uncertain composite wing illustrated in **Figure 2**. The deterministic design maximizes flutter speed. When this design is re-evaluated probabilistically, mode switching leads to bimodal behavior and large POFs for design speeds well below the deterministic flutter speed (i.e., 38% POF for a design speed of 150 m/s). The two reliability-based designs in the figure (which minimize the probability that an instability will occur below some design speed) remedy this issue: The optimal PDFs are unimodal in nature with reasonably low POFs, albeit with inferior deterministic flutter speeds.

This example from Scarth et al. (2015) utilizes TAE systems for flutter prediction. One may also expect severe complications related to discontinuous flutter surfaces and multimodal PDFs for a transonic aeroelastic case with strong shock behavior (e.g., **Figure 3**). However, the use of CAE for an RBDO problem of this nature is beyond the current state of the art, given the large number of function evaluations needed both to approximate the Gaussian process and to conduct

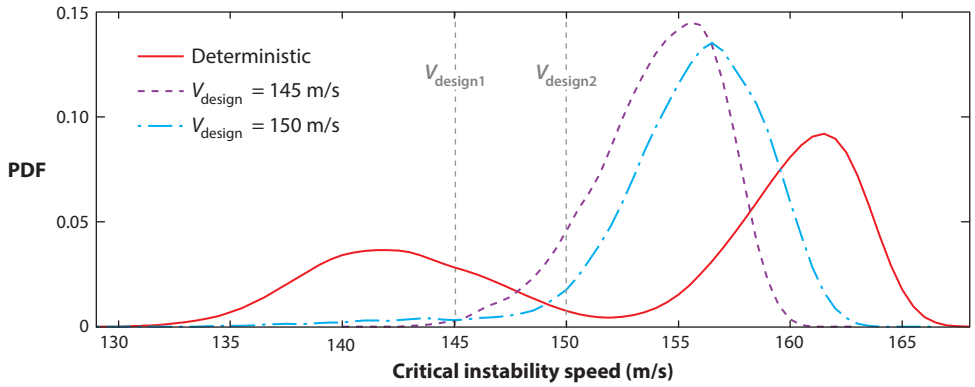

Figure 6

Optimal flutter probability density functions (PDFs) for a deterministic design (maximum flutter speed) and two probabilistic designs (which maximize the probability that the flutter speed will be above a set design speed). Figure adapted from Scarth et al. (2015) with permission of the American Institute of Aeronautics and Astronautics, Inc.

the non-gradient-based optimization, and also because FORM (which can generally be conducted in a CAE environment) will be inaccurate owing to the bimodal PDF.

SP: sigma point

4.2. Robust Design Optimization

The inclusion of robustness metrics (about the mean of a PDF) in aeroelastic optimization is not as prevalent in the literature as reliability metrics (within the tails of a PDF). Robustness is more concerned with aeroelastic performance (such as the lift-to-drag ratio), rather than failure mechanisms such as flutter. One method of RDO is to maximize the probability that the performance will be greater than the deterministic performance, such as done by Allen & Maute (2004) for the cruise efficiency of a wing. This probability can be computed with FORM. The direct inclusion of the mean and standard deviation of an objective function, as written in Equation 9, is more complex. Perturbation methods suffer from the same deficiencies as SORM, in that second derivatives are needed to estimate μ_f and σ_f, although only the diagonal of the Hessian is needed for the mean (Verhoosel et al. 2009).

Other authors have employed Gaussian quadrature formulas to compute robustness metrics. For example, Paiva et al. (2014) utilized the sigma point (SP) method to estimate μ_f and σ_f of the cruise lift-to-drag ratio of a flexible wing, a weighted combination of which is minimized for RDO (the authors considered reliability-based stress constraints as well). The SP method requires $2n+1$ samples to compute (via a Gaussian quadrature) μ_f and σ_f but does not depend on the derivatives with respect to $\mathbf{r}$ (unlike the perturbation methods). Furthermore, design derivatives of μ_f and σ_f with respect to $\mathbf{x}$ are readily available via analytical differentiation at each sample point. Provided the number of RVs is moderate, the SP method (or any of the like-minded Gaussian quadrature formulas surveyed in Padulo et al. 2011, with varying computational cost and accuracy) is a viable choice for CAE-based RDO, although it has not, to our knowledge, been utilized as such.

PCE may also be used for CAE-based RDO, with moment derivatives with respect to $\mathbf{x}$ (for gradient-based optimization) formulated by Eldred (2009). As above, to our knowledge, no CAE examples of this process are available in the literature, although Rallabhandi et al. (2015) provided a recent CFD-based aerodynamic RDO example. As noted, PCE sampling requirements may be alleviated with sparse regularized expansions (Blatman & Sudret 2010) or gradient enhancements (Roderick et al. 2010). The latter technique is complicated in the case of nondeterministic design variables, as second-order derivatives may be required for RDO. A global surrogate model such as PCE is perhaps the only option when a multimodal response PDF exists, although this situation may be less likely for performance-based RDO, as opposed to failure-driven (i.e., flutter) RBDO.

5. CONCLUSION

Quantifying uncertainties in aeroelasticity is important for the development of safe, efficient, and highly capable aircraft. To gain a perspective on the selection, application, and limitations of appropriate UQ methods, above we review literature from the TAE and CAE communities, covering the analysis and design of aerospace structures. UQ methods based on nondeterministic sampling, spectral expansions and response surfaces, stochastic collocation, classification, and perturbation analysis are discussed, with commentary on method efficiency, the ability to capture system behaviors, and relevance to optimization.

There are three broad challenges for UQ in aeroelasticity: discontinuous responses, high computational costs, and potentially complex physics. Quantifying sources of uncertainty is also a key challenge, but outside the scope of this review. With regard to the first challenge, discontinuous responses correspond to bifurcations and folds in solution surfaces and/or switching of failure

modes (occurring even when the aerodynamic model is linear) in the design space. In future UQ-based TAE and CAE assessments, we anticipate the increased utility of probabilistic methods attuned to the capture of discontinuous failure surfaces (potentially forming a disjointed set), such as support vector machine (e.g., see Basudhar & Missoum 2013 regarding the probability of misclassification or Devathi et al. 2016 regarding a reliability analysis framework accounting for misclassification), adaptively sampled Gaussian process models (Bichon et al. 2008), or adaptive stochastic collocation (Dwight et al. 2013).

The second challenge, high computational cost, is a barrier to applying UQ approaches to CFD-oriented CAE models. These models, often involving millions of state variables, are typically solved in the time domain over large periods with relatively small steps. Although the steadily increasing availability of computing resources will help, analysis-oriented techniques are also attractive to mitigate these costs: (*a*) nonlinear time-periodic methods that reduce the simulation time by avoiding a general transient analysis (Hayes & Marques 2015); (*b*) a Schur complement approach to condense the influence of aerodynamic variables (Marques et al. 2010, Timme et al. 2010); (*c*) linearized time-domain and harmonic methods geared toward fast flutter prediction (Bhatia & Beran 2014, 2015); (*d*) reduced-order modeling techniques to construct and solve compact aeroelastic models (Dowell & Hall 2001, Beran et al. 2004b, Lucia et al. 2004), which become sources of modeling uncertainty, and (*e*) heightened parallelization of CAE methods to apply greater computational resources to individual analyses.

UQ in CAE will also itself require more efficient methods. To begin, there is a need for practical methods for parameter spaces of dimensionality greater than $\mathcal{O}(10^3)$, especially when the cost of generating samples is high and the space potentially features complex distributions of failure surfaces. This size is driven by the richness of parameter descriptions appearing at the preliminary design stage and the requisite physical couplings, which obstruct decomposition of the optimization problem. Progress in resolving the so-called curse of dimensionality has been slow. Some potential helpful directions include the use of active subspaces to expose key parameters in the forward UQ problem (Constantine et al. 2014), adjoint-based sensitivity analysis methods to enable more efficient gradient-enhanced response surfaces (Roderick et al. 2010) in a manner that scales better with increased dimensionality, and adaptive sampling methods that operate in parallel. Finally, we note that UQ methods are often enabled by parametric model representations amenable to automated use; this is not often the case in CAE practice.

A third challenge to UQ in aeroelastic systems is the modeling of physical complexity. Aeroelastic interactions distribute, and potentially exacerbate, the influence of sources of uncertainty across the coupled system in unexpected ways. Important dynamical couplings are numerous: F-16 LCO impacted by shock-induced trailing-edge separation (Cunningham 1998), the buffet of tails in a vortical wash (Komerath et al. 1992), the buffet of wings in the presence of vortex breakdown (Gordnier & Visbal 2004), and the quenching of wing LCOs by vortices (Gordnier & Melville 1999). All these interactions may lead to chaotic responses not amenable to conventional sensitivity analysis (Wang et al. 2014). Even the low-fidelity aerodynamic models typically used in TAE methods complicate the UQ process via multiple competing failure modes (Scarth et al. 2014)—accounting for interactions between the structure and complex aerodynamic physics will only make UQ in CAE more challenging and the interpretation of results more opaque, especially when considering the high cost of individual CAE analyses. Thus, UQ methods should be vetted in application to TAE before being relied on in CAE. We also acknowledge the complexity and physical scales arising from structural sources, including control-surface freeplay (Tang & Dowell 2010) and nonlinear damping (Chen et al. 1998).

There are few solutions to addressing physical complexity when it drives the UQ process. One emerging idea is to take a multifidelity approach: collecting samples with models of different

fidelity. This strategy seeks to minimize the number of high-fidelity analyses, using the information to calibrate lower-fidelity models over a broader portion of the parameter space (e.g., see Timme 2010 for multifidelity CAE or Bryson & Rumpfkeil 2016 for PCE-based approaches). Furthermore, the merging of low- and high-fidelity data provides a natural connection between TAE and CAE, helping to ensure that the wisdom embodied in established engineering models is not lost when making decisions regarding aircraft design or certification, while restricting the use of CAE to situations with greatest impact.

DISCLOSURE STATEMENT

The authors are not aware of any biases that might be perceived as affecting the objectivity of this review.

ACKNOWLEDGMENTS

This work is sponsored by the US Air Force Office of Scientific Research under laboratory task 03VA01COR (monitored by Jean-Luc Cambier), as well as NASA's Advanced Air Transport Technologies Project.

LITERATURE CITED

Allen M, Camberos J. 2009. *Comparison of uncertainty propagation/response surface techniques for two aeroelastic systems*. Presented at AIAA Struct. Struct. Dyn. Mater. Conf., 50th, Palm Springs, CA, AIAA Pap. 2009-2269

Allen M, Maute K. 2004. Reliability-based design optimization of aeroelastic structures. *Struct. Multidiscip. Optim.* 27:228–42

Allen M, Maute K. 2005. Reliability-based shape optimization of structures undergoing fluid–structure interaction phenomena. *Comput. Methods Appl. Mech. Eng.* 194:3472–95

Attar PJ, Dowell EH. 2006. Stochastic analysis of a nonlinear aeroelastic model using the response surface method. *J. Aircr.* 43:1044–52

Badcock KJ, Timme S, Marques S, Khodaparast H, Prandina M, et al. 2011. Transonic aeroelastic simulation for instability searches and uncertainty analysis. *Prog. Aerosp. Sci.* 47:392–423

Bansal P, Pitt D. 2013. *Stochastic variations in aerodynamic influence coefficients (AICs) on flutter prediction of a generic wing*. Presented at AIAA Struct. Struct. Dyn. Mater. Conf., 54th, Boston, MA, AIAA Pap. 2013-1841

Barth T. 2013. Non-intrusive uncertainty propagation with error bounds for conservation laws containing discontinuities. See Bijl et al. 2013, pp. 1–57

Basudhar A, Missoum S. 2013. Reliability assessment using probabilistic support vector machines. *Int. J. Reliab. Saf.* 7:156–73

Bendiksen OO. 2006. *Non-Hopfian transonic flutter*. Presented at ASME 2006 Pressure Vessels Piping/ICPVT-11 Conf., PVP2006-ICPVT-11-93960

Bendiksen OO. 2009. High-altitude limit cycle flutter of transonic wings. *J. Aircr.* 46:123–36

Beran PS, Khot NS, Eastep FE, Snyder RD, Zweber JV. 2004a. Numerical analysis of store-induced limit-cycle oscillation. *J. Aircr.* 41:1315–26

Beran PS, Lucia D, Pettit CL. 2004b. Reduced-order modelling of limit-cycle oscillation for aeroelastic systems. *J. Fluids Struct.* 19:575–90

Beran PS, Pettit CL. 2004. *A direct method for quantifying limit-cycle oscillation response characteristics in the presence of uncertainties*. Presented at AIAA Struct. Struct. Dyn. Mater. Conf., 45th, Palm Springs, CA, AIAA Pap. 2004-1695

Beran PS, Pettit CL, Millman DR. 2006. Uncertainty quantification of limit-cycle oscillations. *J. Comput. Phys.* 217:217–47

Beran PS, Stanford B. 2013. Uncertainty quantification in aeroelasticity. See Bijl et al. 2013, pp. 59–103
Bhatia M, Beran P. 2014. *Higher-order transonic flutter solutions*. Presented at AIAA Struct. Struct. Dyn. Mater. Conf., 55th, National Harbor, MD, AIAA Pap. 2014-0336
Bhatia M, Beran P. 2015. *h*-Adaptive stabilized finite-element solver for calculation of generalized aerodynamic forces. *AIAA J.* 53:554–72
Bichon BJ, Eldred MS, Swiler LP, Mahadevan S, McFarland JM. 2008. Efficient global reliability analysis for nonlinear implicit performance functions. *AIAA J.* 46:2459–68
Bijl H, Lucor D, Mishra S, Schwab C, eds. 2013. *Uncertainty Quantification in Computational Fluid Dynamics*. Lect. Notes Comput. Sci. Eng. 92. New York: Springer
Bisplinghoff RL, Ashley H, Halfman RL. 1955. *Aeroelasticity*. New York: Addison-Wesley
Blatman G, Sudret B. 2010. An adaptive algorithm to build up sparse polynomial chaos expansions for stochastic finite element analysis. *Probab. Eng. Mech.* 25:1831–97
Bryson DE, Rumpfkeil MP. 2016. *Variable-fidelity surrogate modeling of lambda wing transonic aerodynamic performance*. Presented at AIAA Aerosp. Sci. Meet., 54th, San Diego, CA, AIAA Pap. 2016-0294
Bunton RW, Denegri CM. 2000. Limit cycle oscillation characteristics of fighter aircraft. *J. Aircr.* 37:916–18
Caracoglia L. 2013. An Euler–Monte Carlo algorithm assessing moment Lyapunov exponents for stochastic bridge flutter predictions. *Comput. Struct.* 122:65–77
Castravete SC, Ibrahim RA. 2008. Effect of stiffness uncertainties on the flutter of a cantilever wing. *AIAA J.* 46:925–35
Chen P, Sarhaddi D, Liu D. 1998. *Limit-cycle oscillation studies of a fighter with external stores*. Presented at AIAA Struct. Struct. Dyn. Mater. Conf., 39th, Long Beach, CA, AIAA Pap. 1998-1727
Constantine PG, Dow E, Wang Q. 2014. Active subspace methods in theory and practice: applications to Kriging surfaces. *SIAM J. Sci. Comput.* 36:A1500–24
Cunningham A. 1998. *The role of non-linear aerodynamics in fluid-structure interaction*. Presented at AIAA Fluid Dyn. Conf., 29th, Albuquerque, NM, AIAA Pap. 1998-2423
Dai Y, Yang C. 2014. Methods and advances in the study of aeroelasticity with uncertainties. *Chin. J. Aeronaut.* 27:461–74
Denegri CM, Dubben JA, Kernazhitskiy SL. 2013. Underwing missile aerodynamic effects on flight-measured limit-cycle oscillations. *J. Aircr.* 50:1637–45
Devathi H, Hu Z, Mahadevan S. 2016. *Modeling epistemic uncertainty in the representation of spatial and temporal variability in reliability analysis*. Presented at AIAA Non-Deterministic Approaches Conf., 18th, San Diego, CA, AIAA Pap. 2016-1677
Dowell EH. 2015. *A Modern Course in Aeroelasticity*. New York: Springer. 5th rev. ed.
Dowell EH, Edwards J, Strganac T. 2003. Nonlinear aeroelasticity. *J. Aircr.* 40:857–74
Dowell EH, Hall KC. 2001. Modeling of fluid-structure interaction. *Annu. Rev. Fluid Mech.* 33:445–90
Dwight RP, Witteveen JA, Bijl H. 2013. Adaptive uncertainty quantification for computational fluid dynamics. See Bijl et al. 2013, pp. 151–91
Eldred M. 2009. *Recent advances in non-intrusive polynomial chaos and stochastic collocation methods for uncertainty analysis and design*. Presented at AIAA Struct. Struct. Dyn. Mater. Conf., 50th, Palm Springs, CA, AIAA Pap. 2009-2274
Eldred M, Burkardt J. 2009. *Comparison of non-intrusive polynomial chaos and stochastic collocation methods for uncertainty quantification*. Presented at AIAA Aerosp. Sci. Meet., 47th, Orlando, FL, AIAA Pap. 2009-976
Farhat C, Geuzaine P, Brown G. 2003. Application of a three-field nonlinear fluid–structure formulation to the prediction of the aeroelastic parameters of an F-16 fighter. *Comput. Fluids* 32:3–29
Friedmann PP, Hodges DH. 2003. Rotary wing aeroelasticity: a historical perspective. *J. Aircr.* 40:1019–46
Georgiou G, Manan A, Cooper J. 2012. Modeling composite wing aeroelastic behavior with uncertain damage severity and material properties. *Mech. Syst. Signal. Proc.* 32:32–43
Ghanem RG, Spanos PD. 1991. *Stochastic Finite Elements: A Spectral Approach*. New York: Springer-Verlag
Ghommem M, Hajj MR, Nayfeh AH. 2010. Uncertainty analysis near bifurcation of an aeroelastic system. *J. Sound. Vib.* 329:3335–47
Gordnier R, Melville R. 1999. *Physical mechanisms for limit-cycle oscillations of a cropped delta wing*. Presented at Fluid Dyn. Conf., 30th, Norfolk, VA, AIAA Pap. 1999-3796

Gordnier R, Visbal M. 2004. Computation of the aeroelastic response of a flexible delta wing at high angles of attack. *J. Fluids Struct.* 19:785–800

Hammersley J, Handscomb D. 1964. *Monte Carlo Methods*. London: Methuen & Co.

Hassig HJ. 1971. An approximate true damping solution of the flutter equation by determinant iteration. *J. Aircr.* 8:885–89

Hayes R, Marques SP. 2015. Prediction of limit cycle oscillations under uncertainty using a harmonic balance method. *Comput. Struct.* 148:1–13

Hayes R, Marques SP, Yao W. 2014. *Analysis of transonic limit cycle oscillations under uncertainty*. Presented at R. Aeronaut. Soc. Aircr. Struct. Des. Conf., 4th, Belfast

Hosder S, Walters R, Balch M. 2008. *Efficient uncertainty quantification applied to the aeroelastic analysis of a transonic wing*. Presented at AIAA Aerosp. Sci. Meet. Exhib., 46th, Reno, NV, AIAA Pap. 2008-729

Khodaparast HH. 2010. *Stochastic finite element model updating and its application in aeroelasticity*. PhD Thesis, Univ. Liverpool

Khodaparast HH, Mottershead JE, Badcock KJ. 2010. Propagation of structural uncertainty to linear aeroelastic stability. *Comput. Struct.* 88:223–36

Komerath NM, Schwartz RJ, Kim JM. 1992. Flow over a twin-tailed aircraft at angle of attack. II. Temporal characteristics. *J. Aircr.* 29:553–58

Kunz DL. 2005. Analysis of proprotor whirl flutter: review and update. *J. Aircr.* 42:172–78

Kurdi M, Lindsley N, Beran P. 2007. *Uncertainty quantification of the Goland$^+$wing's flutter boundary*. Presented at AIAA Atmos. Flight Mech. Conf., Hilton Head, SC, AIAA Pap. 2007-6309

Lamorte N, Friedmann PP, Glaz B, Culler AJ, Crowell AR, McNamara JJ. 2014. Uncertainty propagation in hypersonic aerothermoelastic analysis. *J. Aircr.* 51:192–203

Le Maître OP, Knio OM, Najm HN, Ghanem RG. 2001. A stochastic projection method for fluid flow: I. Basic formulation. *J. Comput. Phys.* 173:481–511

Liaw D, Yang HT. 1991. Reliability of uncertain laminated shells due to buckling and supersonic flutter. *AIAA J.* 29:1698–708

Lindsley NJ, Beran PS, Pettit CL. 2006a. *Integration of model reduction and probabilistic techniques with deterministic multi-physics models*. Presented at AIAA Aerosp. Sci. Meet. Exhib., 44th, Reno, NV, AIAA Pap. 2006-192

Lindsley NJ, Pettit CL, Beran PS. 2006b. Nonlinear plate aeroelastic response with uncertain stiffness and boundary conditions. *Struct. Infrastruct. Eng.* 2:201–20

Livne E. 2003. Future of airplane aeroelasticity. *J. Aircr.* 40:1066–92

Lucia DJ, Beran PS, Silva WA. 2004. Reduced-order modeling: new approaches for computational physics. *Prog. Aerosp. Sci.* 40:51–117

Manan A, Cooper J. 2009. Design of composite wings including uncertainties: a probabilistic approach. *J. Aircr.* 46:601-7

Mani K, Mavriplis DJ. 2008. Unsteady discrete adjoint formulation for two-dimensional flow problems with deforming meshes. *AIAA J.* 46:1351–64

Mantegazza P, Bindolino G. 1987. Aeroelastic derivatives as a sensitivity analysis of nonlinear equations. *AIAA J.* 25:1145–46

Marques S, Badcock KJ, Khodaparast HH, Mottershead JE. 2010. Transonic aeroelastic stability predictions under the influence of structural variability. *J. Aircr.* 47:1229–39

Melchers RE. 1987. *Structural Reliability*. Chichester, UK: Horwood

Millman DR. 2004. *Quantifying initial condition and parametric uncertainties in a nonlinear aeroelastic system with an efficient stochastic algorithm*. PhD Thesis, Air Force Inst. Technol., Wright-Patterson Air Force Base, OH

Millman DR, King PI, Beran PS. 2005. Airfoil pitch-and-plunge bifurcation behavior with Fourier chaos expansions. *J. Aircr.* 42:376–84

Millman DR, King PI, Maple RC, Beran PS, Chilton LK. 2006a. Estimating the probability of failure of a nonlinear aeroelastic system. *J. Aircr.* 43:504–16

Millman DR, King PI, Maple RC, Beran PS, Chilton LK. 2006b. Uncertainty quantification with a B-spline stochastic projection. *AIAA J.* 44:1845–53

Missoum S, Dribusch C, Beran P. 2010. Reliability-based design optimization of nonlinear aeroelasticity problems. *J. Aircr.* 47:992–98

Morton SA, Beran PS. 1999. Hopf-bifurcation analysis of airfoil flutter at transonic speeds. *J. Aircr.* 36:421–29

Murugan S, Harusampath D, Ganguli R. 2008. Material uncertainty propagation in helicopter nonlinear aeroelastic response and vibration analysis. *AIAA J.* 46:2332–44

Najm HN. 2009. Uncertainty quantification and polynomial chaos techniques in computational fluid dynamics. *Annu. Rev. Fluid Mech.* 41:35–52

Nav. Air Syst. Command. 1993. *Airplane strength and rigidity, vibration, flutter, and divergence*. Mil. Specif. MIL-A-8870C, Nav. Air Syst. Command, Dep. Navy

Nikbay M, Acar P. 2015. *Multidisciplinary uncertainty quantification in aeroelastic analyses of semi-span supersonic transport wing*. Presented at AIAA Multidiscip. Anal. Optim. Conf., 16th, AIAA Pap. 2015-3441

Nikbay M, Kuru MN. 2013. Reliability based multidisciplinary optimization of aeroelastic systems with structural and aerodynamic uncertainties. *J. Aircr.* 50:708–15

Oberkampf WL, Roy CJ. 2010. *Verification and Validation in Scientific Computing*. Cambridge, UK: Cambridge Univ. Press

Padulo M, Campobasso MS, Guenov MD. 2011. Novel uncertainty propagation method for robust aerodynamic design. *AIAA J.* 49:530–43

Paiva RM, Crawford C, Suleman A. 2014. Robust and reliability-based design optimization framework for wing design. *AIAA J.* 52:711–24

Pettit CL. 2004. Uncertainty quantification in aeroelasticity: recent results and research challenges. *J. Aircr.* 41:1217–29

Pettit CL, Beran PS. 2004. *Polynomial chaos expansion applied to airfoil limit cycle oscillations*. Presented at AIAA Struct. Struct. Dyn. Mater. Conf., 45th, Palm Springs, CA, AIAA Pap. 2004-1691

Pettit CL, Grandhi RV. 2003. Optimization of a wing structure for gust response and aileron effectiveness. *J. Aircr.* 40:1185–91

Rackwitz R. 2001. Reliability analysis—a review and some perspectives. *Struct. Saf.* 23:365–95

Rallabhandi S, West T, Nielsen E. 2015. *Uncertainty analysis and robust design of low-boom concepts using atmospheric adjoints*. Presented at AIAA Appl. Aerodyn. Conf., 33rd, Dallas, TX, AIAA Pap. 2015-2582

Reed B. 1981. *Flutter at a Glance*. NASA Tech. Film Serial L-1274, NASA, Washington, DC

Riley ME. 2011. *Quantification of model-form, predictive, and parametric uncertainties in simulation-based design*. PhD Thesis, Wright State Univ., Dayton, OH

Riley ME, Grandhi RV, Kolonay R. 2011. Quantification of modeling uncertainty in aeroelastic analyses. *J. Aircr.* 48:866–73

Roache PJ. 1997. Quantification of uncertainty in computational fluid dynamics. *Annu. Rev. Fluid Mech.* 29:123–60

Roderick O, Anitescu M, Fischer P. 2010. Polynomial regression approaches using derivative information for uncertainty quantification. *Nucl. Sci. Eng.* 164:122–39

Sarkar S, Witteveen JAS, Loeven A, Bijl H. 2009. Effect of uncertainty on the bifurcation behavior of pitching airfoil stall flutter. *J. Fluids Struct.* 25:304–20

Scarth C, Cooper JE, Weaver PM, Silva GHC. 2014. Uncertainty quantification of aeroelastic stability of composite plate wings using lamination parameters. *Compos. Struct.* 116:84–93

Scarth C, Sartor P, Cooper J, Weaver P, Silva G. 2015. *Robust aeroelastic design of a composite wing-box*. Presented at AIAA Non-Deterministic Approaches Conf., 17th, Kissimmee, FL, AIAA Pap. 2015-0918

Stanford B, Beran P. 2012. Computational strategies for reliability-based structural optimization of aeroelastic limit cycle oscillations. *Struct. Multidiscip. Optim.* 45:83–99

Stanford B, Beran P. 2013a. Direct flutter and limit cycle computations of highly flexible wings for efficient analysis and optimization. *J. Fluids Struct.* 36:111–23

Stanford B, Beran P. 2013b. Minimum-mass panels under probabilistic aeroelastic flutter constraints. *Finite Element Anal. Des.* 70–71:15–26

Tang D, Dowell EH. 2010. Aeroelastic airfoil with free play at angle of attack with gust excitation. *AIAA J.* 48:427–42

Thomas J, Dowell E, Hall K, Denegri C. 2006. *An investigation of the sensitivity of F-16 fighter flutter onset and limit cycle oscillations to uncertainties*. Presented at AIAA Struct. Struct. Dyn. Mater. Conf., 47th, Newport, RI, AIAA Pap. 2006-1847

Timme S. 2010. *Transonic aeroelastic instability searches using a hierarchy of aerodynamic models*. PhD Thesis, Univ. Liverpool

Timme S, Badcock KJ. 2009. Oscillatory behavior of transonic aeroelastic instability boundaries. *AIAA J.* 47:1590–92

Timme S, Badcock KJ. 2010. *Searching for transonic aeroelastic instability using an aerodynamic model hierarchy*. Presented at AIAA/ASME/ASCE/AHS/ASC Struct. Struct. Dyn. Mater. Conf., 51st, Orlando, FL, AIAA Pap. 2010-3048

Timme S, Marques S, Badcock K. 2010. *Transonic aeroelastic stability analysis using a Kriging-based Schur complement formulation*. Presented at AIAA Atmos. Flight Mech. Conf., Toronto, AIAA Pap. 2010-8228

Verhoosel CV, Scholcz TP, Hulshoff SJ, Gutiérrez MA. 2009. Uncertainty and reliability analysis of fluid-structure stability boundaries. *AIAA J.* 47:91–104

Wang Q, Hu R, Blonigan P. 2014. Least squares shadowing sensitivity analysis of chaotic limit cycle oscillations. *J. Comput. Phys.* 267:210–24

Witteveen JA. 2009. *Efficient and robust uncertainty quantification for computational fluid dynamics and fluid-structure interaction*. PhD Thesis, Delft Univ. Technol.

Xiu D, Karniadakis G. 2002. The Wiener-Askey polynomial chaos for stochastic differential equations. *SIAM J. Sci. Comput.* 24:619–44

Xiu D, Lucor D, Su CH, Karniadakis GM. 2002. Stochastic modeling of flow-structure interactions using generalized polynomial chaos. *J. Fluids Eng.* 124:51–59

Yao W, Chen X, Luo W, van Tooren M, Guo J. 2011. Review of uncertainty-based multidisciplinary design optimization methods for aerospace vehicles. *Prog. Aerosp. Sci.* 47:450–79

Yates EC. 1988. *Agard standard aeroelastic configurations for dynamic response I—wing 445.6*. AGARD Rep. 265, NATO, Brussels

Yi L, Zhichun Y. 2010. Uncertainty quantification in flutter analysis for an airfoil with preloaded freeplay. *J. Aircr.* 47:1454–57

Zang TA, Hemsch MJ, Hilburger MW, Kenny SP, Luckring JM, et al. 2002. *Needs and opportunities for uncertainty-based multidisciplinary design methods for aerospace vehicles*. Tech. Rep. TM-2002-211462, NASA Langley Res. Cent., Hampton, VA

Zhang Z, Chen PC, Wang X, Mignolet MP. 2016. *Nonlinear aerodynamics and nonlinear structures interaction for F-16 limit cycle oscillation prediction*. Presented at Dyn. Specialists Conf., 15th, AIAA Pap. 2016-1796